Distribution Agreement

In presenting this thesis or dissertation as a partial fulfillment of the requirements for an advanced degree from Emory University, I hereby grant to Emory University and its agents the non-exclusive license to archive, make accessible, and display my thesis or dissertation in whole or in part in all forms of media, now or hereafter known, including display on the world wide web. I understand that I may select some access restrictions as part of the online submission of this thesis or dissertation. I retain all ownership rights to the copyright of the thesis or dissertation. I also retain the right to use in future works (such as articles or books) all or part of this thesis or dissertation.

Signature:

_____   _____

Amanda Riana Arulpragasam   Date

Dorsal anterior cingulate and anterior insula encode a novel subjective value prediction
error signal during effort-based decision-making

By

Amanda R. Arulpragasam
Master of Arts

Clinical Psychology

_____
Michael T. Treadway, Ph.D.
Advisor

_____
Scott O. Lilienfeld, Ph.D.
Committee Member

_____
Gregory S. Berns, M.D., Ph.D.
Committee Member

Accepted:

_____
Lisa A. Tedesco, Ph.D.
Dean of the James T. Laney School of Graduate Studies

_____
Date

Dorsal anterior cingulate and anterior insula encode a novel subjective value prediction
error signal during effort-based decision-making

By

Amanda Riana Arulpragasam
B.S., B.A., Duke University, 2012

Advisor: Michael T. Treadway, Ph.D.

An abstract of a thesis submitted to the faculty of the
James T. Laney School of Graduate Studies of Emory University
in partial fulfillment of the requirements for the degree of
Master of Arts in Psychology
2017

Abstract

Dorsal anterior cingulate and anterior insula encode a novel subjective value prediction error signal during effort-based decision-making

By Amanda Riana Arulpragasam

Integrating cost and benefit information is crucial for optimal decision-making. The dorsal anterior cingulate cortex (dACC) and anterior insula (AI) have been implicated in effort-based decision-making, but it remains unknown whether computations performed by these regions are involved in the evaluation of effort, reward, or their integration. To this end, 28 healthy participants completed a novel sequential effort-based decision-making task while undergoing functional magnetic resonance imaging (fMRI). This task presented trial-wise information about effort costs and reward magnitude separately throughout time, allowing us to model distinct effort-based choice computations. We observed a role for dACC in subjective value discounting and choice difficulty, but not for effort cost encoding. Notably, we observed a novel role for dACC in the generation of subjective value prediction error signals as choice-relevant information unfolded. We also observed co-activation of AI with dACC as part of a network unique to this prediction error. These data help elucidate multiple computations performed by dACC during effort-based decision-making as well as provide evidence for the recruitment of AI to aid in prediction error signaling .

Dorsal anterior cingulate and anterior insula encode a novel subjective value prediction
error signal during effort-based decision-making

By

Amanda Riana Arulpragasam
B.S., B.A., Duke University, 2012

Advisor: Michael T. Treadway, Ph.D.

A thesis submitted to the faculty of the
James T. Laney School of Graduate Studies of Emory University
in partial fulfillment of the requirements for the degree of
Master of Arts in Psychology
2017

Table of Contents

Introduction

Optimally weighing the benefits of potential rewards against the effort required to achieve them underlies successful decision-making and foraging behavior[1-3]. Across species, studies have demonstrated that cost/benefit options requiring greater effort are perceived as having lower subjective value compared to options requiring less effort[4,5]. It remains unclear, however, exactly how the brain performs effort-based decision computations through time.

Two brain areas previously implicated in effort-based decision-making are the medial prefrontal cortex (mPFC), specifically the dorsal anterior cingulate cortex (dACC), and the anterior insula (AI). Both these regions have been found to encode effort costs as well as the subjective value of decision options. Lesions to the mPFC have routinely been found to induce a shift in preference away from larger rewards requiring greater effort in favor of lower effort options in rodents[6-10], with similar effects observed from dACC lesions in primates[6,11,12]. Electrophysiological recordings of single cell activity have also found dACC to be one of the only prefrontal areas to be sensitive to effort costs[13-17]. Similarly, in tasks requiring physical effort, AI has been shown to co-activate with dACC as effort costs increase, possibly suggesting a primary role for AI in encoding effort-related costs[18-21]. Further, both animal and neuroimaging studies have demonstrated that subjective values are represented in distinct brain areas including the ACC and anterior insular cortices for physical effort[11,19].

Importantly, these regions also play a role in learning and prediction updating. In neuroimaging studies of effort based decision-making in humans, dACC has been found to encode both signed and unsigned prediction errors[22-24]. AI has also been implicated in encoding negative prediction errors[25] as well as cost prediction signals, that is, predictions about future cost requirements[26].

Consequently, it remains unclear what specific computations, such as effort cost encoding or updating, these regions perform in the context of effort-based decisions. The dACC is among the most commonly activated brain areas across tasks, leading to a variety of theoretical accounts regarding its general function[27-34]. These have included error detection[35], conflict monitoring[36], and value-based decision-making[27,29,37]. In the context of the latter, the dACC has been shown to monitor the value of less favored and/or unchosen options[38], provide a "boosting signal" to overcome those response costs[39], or reflect the difficulty of determining the best choice among two nearly-equivalent options[31,34]. Similarly, the precise role of the insula in effort-related decisions remains unclear. Like dACC, the insula is associated with a variety of functions including encoding aversive outcomes, risk[26], and processing pain.

One challenge to evaluating the role of both dACC and AI computations during effort-based decisions has been the use of task paradigms that provide information about costs and reward simultaneously[40]. To better isolate the role for these regions in computations of effort cost, subjective value, choice difficulty, and prediction error signaling, we used a sequential effort-based decision-making task where trial-wise information about effort

costs and reward were presented separately throughout time, allowing us to model

distinct computations related to effort cost encoding, subjective value, choice difficulty,

and prediction error. We observed a role for dACC across all modeled computations with

the exception of effort cost encoding. Interestingly, we only observed a role for AI as part

of a network for subjective value error signaling. These data help elucidate multiple,

distinct computations performed by dACC during effort-based decision-making and well

as evidence for the recruitment of AI to aid in prediction and prediction error-based

processes.

Results

Behavioral Results

Participants performed choices between options with varying rewards and physical

efforts (rapid button pressing). In this task, participants decided whether to choose a "No

Effort Option" for $1.00 or an "Effort Option" requiring some level of physical effort

(rapid button pressing) in exchange for monetary rewards of varying magnitude. The

higher effort option independently varied in required button press rate (effort) and reward

magnitude. The reward magnitude was shown as a dollar amount (range: $1 – $5.73;

based on 4 bins: $1.25- $2.39, $2.40 – $3.49, $3.50 - $4.60, > $4.60) and the required

effort level was indicated as the height of a vertical bar (20%, 50%, 80% or 100% of the

participant's maximum button pressing rate). To examine neural correlates of effort and

reward information separately, information about the effort and reward available for the

"Effort Option" for each trial was presented sequentially. "Effort First" trials began with

an initial presentation of effort required for the Effort Option, followed by the available

reward, while "Reward First" trials had the opposite presentation order. Each trial was

therefore comprised of an initial cue ("Cue 1"), followed by a second cue ("Cue 2"),

which was then followed by a prompt to decide between the Effort Option and the No

Effort Option ("Decision Prompt") at which point subjects made a button press indicating

their selection ("Choice Phase") (**Figure 1A**).

We first tested whether both the size of the reward and the required effort of each choice

option had an impact on participant's choice behavior. A 4 (Effort level) x 4 (reward

magnitude, binned) repeated-measures ANOVA revealed that participants' choices were

strongly guided by both the required effort ($F_{(1.45,39.10)} = 64.27$, $p = 1.74$ x 10^{-11}, partial η^2

$= 0.70$; **Figure 1B**), as well as the reward magnitude of both options ($F_{(2.02,54.47)} = 106.03$,

$p = 1.42$ x 10^{-19}, partial $\eta^2 = 0.80$; **Figure 1B**). There was also an effort x reward

interaction ($F_{(4.40,118.76)} = 8.88$, $p = 0.000001$, partial $\eta^2 = 0.25$**).** As expected, larger

rewards and smaller effort costs attracted more effortful choices. Overall, participants

chose the higher effort option on $66\% \pm 18\%$ of trials.

Computational Model

To better estimate how effort and reward influenced individuals' choices, we used a two-

parameter effort discounting model that had been previously shown to fit effort-based

choices[41] (see Methods for details). Consistent with prior results, this model showed a

superior fit (determined by AIC values) when compared to linear, parabolic, and

hyperbolic discounting models (**Table 1**). Individual and group subjective value model

curves are shown in **Figure 1C**.

Neuroimaging Results

We were interested in investigating neural signatures of effort cost encoding, subjective

value, choice difficulty, and prediction error signaling, specifically in the dACC and AI.

We first sought to determine which regions appeared to be tracking the integration of

reward and effort information at Cue 2 (when the second piece of information was

presented). Here we identified a network of regions including the insula, dACC,

supplementary motor area (SMA), and striatum, regions commonly implicated in effort-

based choice, as well as a variety of other functions[2,18-21] (**Supplemental Figure S1).** In

the analyses that follow, we examined associations with model-based regressors related

to subjective value, choice difficulty, and prediction error during Cue 2.

Subjective Value Encoding

To further understand how effort and reward information combined into an integrated

value at Cue 2, a second GLM (GLM2) was used to examine neural regions that encoded

the subjective value of the chosen option. We observed subjective value discounting in

the dACC (x = -8, y = 20, z = 42, t = 4.69, cluster corrected pFWE = 0.001; **Figure 3A**).

We also found that the subjective value of the chosen option positively correlated with

activity in the vmPFC (x = 4, y = 32, z = -8, t = 5.02, cluster corrected pFWE < 0.001;

Figure 3B), consistent with multiple prior studies[29,37]. We did not identify any activations

in the ventral striatum, even at lenient statistical thresholds (p<0.05, uncorrected).

Importantly, a significant debate has arisen as to whether SV encoding in the dACC may

be wholly reducible to choice difficulty. Our study design was not optimized to address

this particular question, but we observed that SV and choice difficulty were highly

collinear (mean r^2 = 0.49) (**Supplemental Figure S3C**). As a result, the current study

was unable to fully disambiguate between dACC involvement in SV and choice difficulty

(for greater discussion of our choice difficulty model please reference *Supplemental*

Methods).

Subjective Value Prediction Error

Recent work has sought to explain the various functions of ACC and AI under the

unifying principle of prediction and prediction error. In this framework, ACC

continuously formulates predictions linking stimuli, actions, and outcomes, and computes

a prediction error which scales with the difference between the predicted and observed

outcome[22-24]. Due to the involvement of both dACC and insula in learning updating as

well as prediction signals, we modeled trial-based predictions and computed expectation

differentials using a sliding window analysis (GLM3). For example, when subjects saw a

large reward value at Cue 1, they would likely expect a high SV for the trial as a whole

given the ultimate SV of past trials that began with a large reward. However, they could

be "surprised" by a high effort requirement presented at Cue 2, resulting in a negative

subjective value prediction error (SVPE). Our design allowed us to calculate unsigned

prediction errors based on the absolute value of the difference between the observed

subjective value and the predicted trial-wise subjective value after receiving only the first

piece of information. We observed that this modeled prediction error was positively

associated with dACC (x = 8, y = 24, z = 32, t = 4.52, cluster corrected pFWE < 0.001),

caudate (x = 12, y = 2, z = 12, t = 4.18, cluster corrected pFWE = 0.006), and insula (x =

-36, y = 16, z = -10, t = 6.26, cluster corrected pFWE < 0.001) activity, suggesting a role

for these regions in the encoding of unsigned prediction error signals during effort-based

choice (**Figure 3D**). These results remained even when controlling for regressors related

to choice difficulty, subjective value, and choice outcome (Effort or No Effort),

suggesting that the involvement of these regions could not be better explained by these

other processes. Further, our subjective value prediction error regressor was not highly

correlated with any of our other variables of interest (**Supplemental Figure S3A** and

S3B).

Spatial Specificity

To better understand the spatial localization of SVPE and SV signals, we defined ROIs

using previously defined parcellations of dACC, insula, and caudate [42-44] to compare

activity in distinct subregions of these structures. Within dACC, we identified an

anterior/posterior spatial gradient in the encoding of unsigned prediction error signals,

where more anterior subregions of dACC encoded this signal more strongly (**Figure 3D**).

We also observed that dorsal insula more strongly encoded prediction error than ventral

or posterior insula, suggesting spatial specificity for this function (**Figure 3B**). Similarly,

within the caudate, we observed an anterior/posterior spatial gradient, where most

posterior subregions of caudate encoded the SVPE signal more strongly (**Figure 3F**).

Interestingly, this posterior location has been found to encode more executive functions

as opposed to an action or stimulus value[44], which may explain why it is more active for

evaluation expectation differences.

Expectation Formation

The presence of a prediction error at Cue 2, based on the expected SV information presented at Cue 1 suggested that participants were forming expectations at Cue 1, when they only had one piece of information. An advantage of our design is that it allowed us to look neural responses to reward and effort information when presented in isolation (Cue 1). We were interested in exploring subjective responses to the presented options, with the idea that neural structures may be encoding expectations about future effort or reward. While we did not observe any regions that tracked expected effort at Cue 1, we did observe that expected reward at Cue 1 was positively associated with vmPFC activity (x=2, y = 48, z = -8, t = 6.27, cluster corrected pFWE <0.001; **Figure 4),** highlighting this region as essential in forming reward-based predictions. Consistent with the idea that this activity reflected expectations rather than simply encoding of the objective information presented at Cue 1 (i.e., reward magnitude or effort level), we did not identify any regions that significantly responded to the reward magnitude or effort cost of the presented option alone, even at lenient statistical thresholds (p<0.05, uncorrected).

Discussion

The goal of the current study was to investigate areas that were involved in the encoding of effort, reward, and their integration. Human imaging studies as well as animal lesion studies have strongly implicated dACC and AI as critical for effort related decisions, though their function remains unclear. We replicated prior effects relating to effort discounting and choice difficulty in the dACC, and also identified a novel subjective value prediction error signal in the context of effort related decisions.

Early imaging studies have shown a role for dACC in cost encoding, with evidence that

activity in this region scales with increasing effort requirements[19,40]. However, the

present study did not observe these phenomena. Even when looking at presented effort

costs in isolation (i.e., at Cue 1) we did not find evidence that the dACC was encoding

effort cost alone. Rather, the most novel finding in our results was the identification of

dACC involvement in the generation of an unsigned prediction error as choice-relevant

information became available. Our model for SVPE–the absolute value of the difference

between SV of the chosen option and their predicted SV as determined by a sliding

window analysis–is formally similar to a standard unsigned prediction error. While both

signed and unsigned PE signals have previously been identified in dACC in a

reinforcement learning context[22-24], the current result extends this effect to intra-trial

value updating. Interestingly, while dACC appeared to be involved in both SV and

prediction error, AI and caudate were uniquely involved in prediction error signaling (see

Figure 3A and **3E**).

In addition to its role in prediction error generation, we also found evidence that dACC

encoded a *subjective* value such that lower subjective value was associated with elevated

dACC activity, which is consistent with other reports[45]. Further, using a binned trial

analysis (see *Supplemental Methods*), we observed that within a certain choice outcome,

we still observe the SV effect in dACC. Additionally, consistent with previous reports[46],

we observed increasing dACC activity as SV decreases, eventually reaching its peak

when participants must change their strategy and choose the No Effort option. This

suggests that dACC may be implicated in the reevaluation of strategy and that it may, in

our experiment, signal a move away from a "default" preference for the more richly

rewarded Effort Option.

While intriguing, a significant caveat to this interpretation is the role of choice difficulty,

which has been proposed an alternative explanation for dACC engagement[30-34]. Since our

design was not intended to directly address this question, SV was heavily correlated with

choice difficulty (proximity to indifference point). dACC activation in both SV and

choice difficulty analyses revealed substantial overlap in activation clusters. Further,

when both regressors were included, there was no significant activation in dACC for

either. As a result, we cannot determine whether separate SV and choice difficulty signals

exist in dACC, whether the signals represent similar features of a larger process, or

whether one signal can completely account for another. Further research will be required

to disentangle these processes and computations.

Our data also identified a clear role for vmPFC in the context of effort related decisions.

A large number of studies have demonstrated that vmPFC signal scales with expected

reward value across a variety range of reward types[37,47,48]. In the context of effort-

discounting, however, there has been some evidence suggesting a dissociation between

vmPFC and dACC. Animal research has shown that ACC lesions in rats impaired effort

discounting, whereas orbitofrontal cortical lesions only influenced delay discounting[49].

These findings and others suggested that vmPFC does not play a large role in effort-based

decisions. In contrast, we observed that this region had very specific functions as it

related to effort-based decisions. We noted that it encoded the subjective values of the

chosen option as well as the expected or predicted value of available rewards on future trials.

Finally, we also observed engagement of the striatum. Animal studies have identified the striatum, particularly the ventral striatum (VS), as a key region for effort-based decisions[7,25,50-53]. However several recent neuroimaging studies have not observed significant striatal activity during effort-based decision making[54]. We did not detect any significant activation of the ventral striatum, though we did see involvement of the caudate in SVPE signaling. There are several explanations for this discrepancy. First, it should be noted that the vast majority of studies highlighting the ventral striatum in effort-based decision-making have relied on manipulations of dopamine, which was not manipulated here. Dopamine activity in ventral striatum may be necessary for effort-related decisions, but may not necessarily drive striatal activity in this context. Additionally, past research has suggested the ventral striatum represents more of a stimulus value, whereas dorsal striatum more likely encodes action value. It is possible that prior studies allowed for the cognitive decoupling of the value of an option from the cost of obtaining that reward, resulting in greater ventral striatal activity.

Limitations

There are several limitations to the current study that warrant additional comment. First, our sliding window analysis, which underlies our key finding of these regions' involvement in prediction error generation, was not tailored to individual learning rates. That is, our analysis weighted the previous 5 trials at any point for all subjects, but the

amount of weight given to prior trials may have fluctuated both across and within

subjects.

A second limitation is that our participants did not complete effort while they were in the

scanner. Instead, they completed the effort they chose immediately following the scan.

We did present the opportunity for participants to change their responses post-scan to

investigate whether fatigue of performing the effort in real-time might influence

willingness to make effortful choices. We observed near-identical choice patterns post-

scan as we observed during the scan (see Methods). While this may have addressed the

question as to whether fatigue of effort completion influences choice, we cannot be sure

that the act of completing effort in real-time does not change the way participants are

evaluating and making their decisions.

Further, our regressors were not optimally orthogonalized for all relevant questions,

particularly related to subjective value and choice difficulty. While we observed a strong

unsigned subjective value prediction error, our design was not optimized to evaluate a

signed prediction error signal because this regressor would be too highly correlated with

subjective value.

Conclusion

Taken together, our results have identified unique prediction error-based functions within

the context of effort-based decision-making. Going forward, these data help reveal the

precise functions of dACC and AI during effort-based decision-making, and may help

clarify the mechanisms underlying maladaptive decision-making behaviors that are commonly observed in clinical populations such as major depressive disorder[55-57] and schizophrenia[58]. While we predict that these functions generalize to other cost domains outside of effort-based decisions, future studies will be needed to determine the generalizability of these computations to other forms of cost/benefit decision-making (e.g., probability or delay).

Methods

Participants.

Thirty-one healthy volunteers (14 males, M_{age} = 20.8, SD_{age} = 3.4; **Supplemental Table S1**) completed a sequential effort-based decision-making task while undergoing functional magnetic resonance imaging (fMRI). All were right handed, had normal or corrected-to-normal vision, no history of psychiatric or neurological diseases, and no structural brain abnormalities. Of these, three participants were excluded: one for excessive head movement, one for falling asleep, and one for behavioral evidence of inadequate task performance. This yielded datasets from twenty-eight participants (13 males, M_{age} = 20.2, SD_{age} = 2.1) for our final analysis. No statistical tests were used to predetermine sample sizes, but our sample size is within the standard range in the field[2,33,34,38,40,51]. All study procedures were reviewed and approved by the Emory University Institutional review board, and written informed consent was obtained for all participants.

Procedure.

The experimental task was designed to measure independently the neural responses to two dimensions of a cost/benefit decision: the effort required and the magnitude of reward. In this task, participants decided whether to perform a no effort task for $1.00 or a higher effort task for a larger reward of varying magnitude. The higher effort option independently varied in required button press rate (effort) and reward magnitude. The reward magnitude was shown as a dollar amount (range: $1 – $5.73; based on 4 bins: $1.25- $2.39, $2.40 – $3.49, $3.50 - $4.60, > $4.60) and required effort level was indicated as the height of a vertical bar (20%, 50%, 80% or 100% of the participant's maximum button pressing rate). Prior to entering the scanner, participants completed three practice trials where they were asked to press a key with their left pinky finger as quickly as possible for 20 seconds. Participant's maximum effort was calculated based on the average press rate across the three trials. After establishing each participant's maximum button press rate, participants practiced completing 20%, 50%, 80%, and 100% of their maximum effort. As part of this practice, participants completed four trials of each effort level to become familiar with how effortful each value was for them. The practice trials lasted about 5 minutes. Participants were informed that they would not complete the physical effort component while in the scanner, but would have to complete it based on the choices they make immediately following the scan.

Each trial was comprised of a Cue 1, Cue 2, Decision Prompt, and Choice phase. At cue 1, participants were presented with only one piece of information from the higher effort option (either the associated effort level or reward magnitude). Then after a brief, jittered delay of between 2-6 seconds (mean = 2.98s), they saw cue 2, which revealed the other

piece of information. After another brief jittered delay of between 2-6 seconds (mean =

3.23s), the participants were prompted to make their selection: either accept the effortful

option that has been presented or reject that option in favor of the non-effortful option

that pays $1. Then, the participant's selection was shown in the Choice phase. The inter-

stimulus-jitter was drawn from a Poisson distribution, similar to that used in sequential

foraging tasks[38]. Because the non-effortful option was fixed, it was not presented during

the task. Order of information (effort first or reward first), as well as side of presentation

for effort and reward information (right or left) was counterbalanced across trials

(**Figure 1A**). Trials were presented in the same fixed randomized order for all

participants.

While in the scanner, participants completed two runs total of this task. Each run lasted

approximately 9 minutes, and consisted of 44 trials (11 per effort level and reward bin

values). Stimulus presentation and response acquisition was performed using

MatlabR2013b (MathWorks) with the Psychophysics Toolbox[59]. Participants responded

with MR-compatible response keypads.

Following the scan, participants were presented with the effortful options they selected

while in the scanner. They were then asked to complete the effort required for the choices

they had selected. Importantly, for each chosen trial, they were given the opportunity to

change their responses. This option was given to investigate whether fatigue of

performing the effort in real-time might influence willingness to make effortful choices.

We observed very consistent choice patterns post-scan as we observed during the scan, with participants choosing the same options on 97± 4% of trials.

Image acquisition.

Imaging data were acquired on a Siemens 3T Tim Trio using a 32-channel phased-array head coil. Trial presentations were synchronized to initial volume acquisition. Functional (T2* weighted) images were aquired using a multiband sequence with the following sequence parameters: 3-mm^3 isotropic voxels, repetition time (TR) = 1.0 s, echo time (TE) = 30 ms, flip angle (FA) = 65°, 52 interleaved axial slices, with slice orientation tilted 18° relative to the AC/PC plane to improve coverage of ventromedial prefrontal cortex. At the start of the imaging session, a high-resolution structural volume was also collected, with the following sequence parameters: 2-mm × 1-mm × 1-mm voxels, TR = 1.9 s, TE = 2.27 ms, FA = 9°.

Behavioral analysis.

Analyses were conducted using Matlab 2015B (Mathworks, Natick, MA) and SPSS v22 (IBM, Armok, NY). To examine choice data across varying levels of effort and reward magnitude, repeated measures ANOVAs were used. For cases that violated the sphericity assumption, a Greenhouse-Geisser correction was used.

Subjective Value Models

To estimate participants' subjective values for the offers presented on each trial, we used a two-parameter power function, which has been previously described in Klein-Flugge et

al. (2015) [41]. This effort-discounting model has been shown to provide better fits than the

hyperbolic model previously suggested for effort discounting[19] both here and in other

studies[41]. The two-parameter power function estimates subjective values on each trial

using Equation 1, where SV is the subjective value, E is the amount of required effort

(ranging from 0% to 100%), R is the reward magnitude, and k and p are free parameters

that are fit for each participant.

$$SV = R - kE^p \qquad\qquad Eq.\ 1$$

The subjective value of the easy option, which does not require any effort to be exerted

and was always worth \$1, assumes a value of 1 on each trial. Importantly, the p

parameter allows the two-parameter power function to take a concave or convex shape

depending on the rate at which the participant devalues reward with additional effort.

Hyperbolic discounting functions that have been traditionally used for delay discounting

and previously suggested for effort discounting follow a convex function where the

addition of effort has a larger devaluation effect on smaller effort costs and very small

devaluation effects at higher levels of effort. Alternatively, recent work has suggested

that it is both intuitive and biologically plausible for effort discounting to instead take a

concave shape, where additional effort has small effects on subjective value at lower

levels of required effort but increases steeply as effort reaches more demanding levels[41].

To verify that the two-parameter power function provided a better fit for our data, we

compared it to discounting models that use hyperbolic, quadratic, and linear discounting

functions previously used to describe effort discounting[19,60,61]. All models were each fit to

subject's data individually using the MATLAB function *fminsearch* and parameters were

selected for each participant that optimized the likelihood of the behavioral data.

The Softmax function (Equation 2) was used to transform the subjective values of the two

options offered on each trial into choice probabilities for selecting each option, *a*, on trial

t. The Softmax function includes an inverse temperature parameter, β, which is fit as an

additional free parameter for each participant for each of the discounting models. The

inverse temperature parameter determines the degree to which the choice probabilities are

affected by the estimated subjective value of each option, with lower values indicating

random responding and higher values indicating a tendency to choose the option with the

highest SV. The fits of the discounting models were also compared to a simple model that

assumes a fixed probability of choosing each option.

$$P_t(a) = \frac{e^{\beta \cdot SV_a}}{\sum_{i=1}^{2} e^{\beta \cdot SV_i}} \qquad\qquad Eq.\ 2$$

Similar to the two-parameter power model, the hyperbolic discounting model assumes

that participants weigh subjective values of each option, where subjective values are

calculated by devaluing the reward according to the amount of required effort (Equation

3) and compared using the Softmax function. Hyperbolic discounting functions have been

widely used in modeling temporal discounting of rewards[62,63] and have also been

suggested for effort discounting[19,64].

$$SV = \frac{R}{(1+k\mathrm{E})} \qquad\qquad Eq.\ 3$$

The quadratic or parabolic discounting function (Equation 4) is similar to the two-

parameter power function but allows for less flexibility in the shape of the discounting

function. The quadratic discounting function follows a concave shape where the

devaluation of rewards increases with larger effort costs. Quadratic models of effort

discounting have been used to be explain effort-based choice in recent work[45,60].

$$SV = R - kE^2 \qquad\qquad Eq.\ 4$$

The final discounting model that we fit to our data assumes that effort discounting

follows a linear trend—that rewards are discounted at the same rate per additional unit of

effort (Equation 5). The k parameter represents the slope, or rate of discounting, for each

additional unit of effort.

$$SV = R - kE \qquad\qquad Eq.\ 5$$

The additional model that we fit to our data is a fixed probability model. This model

assumes that participants do not systematically integrate reward and effort information to

guide their choices, but instead select each option with a fixed probability that is fit as a

single free parameter. Despite their simplicity, fixed probability models capture base-

rates of responding and can provide a good fit when participants respond with a strong

preference for either option. As such, fixed probability models provide a baseline to

which more sophisticated models can be compared[65].

All models were compared using Akiake's Information Criterion[66] (AIC). AIC provides a method of comparing the relative quality of models that differ in number of free parameters by incorporating goodness of fit (likelihood, L_i) and model complexity (number of free parameters, V_i) using the following equation:

$$AIC_i = -2\ln(L_i) + 2V_i \qquad\qquad \textit{Eq. 6}$$

Thus, the model with the lowest AIC is judged to provide the best fit for the given set of data. The AIC of each model was calculated individually for each participant. The average AIC and average best-fitting parameters for each model are included in **Table 1**.

Subjective Value Prediction Error

Estimates of expected subjective value at Cue 1 ($SV_{predicted}$) were calculated using a sliding window analysis of previously-experienced subjective values of the same trial type. The value of $SV_{predicted}$ on each trial was derived from the Cue 1 stimulus value and recent subjective values of trials with the same stimulus value (i.e. either reward bin or effort level; see *Supplemental Materials* for more information). Subjective values for previous trials were calculated using the two-parameter power function (Equation 1) and each participant's best-fitting parameters. The subjective value prediction error (SVPE) regressor was calculated by subtracting $SV_{predicted}$ from SV_{chosen}, where SV_{chosen} is calculated under the two-parameter power function using the pieces of information provided at both Cue 1 and Cue 2.

fMRI analysis. All neuroimaging data were preprocessed and analyzed in SPM12

(Wellcome Department of Imaging Neuroscience, Institute of Neurology, London, UK).

Preprocessing in SPM12 included realignment estimation and implementation, co-

registration to the individual's high resolution structural scan, normalization to MNI

space, and spatial smoothing using a Gaussian kernel (6mm FWHM). Across all GLMs,

we used the SPM default orthogonalization. When controlling for other regressors, the

regressor of interest was always entered second.

To identify areas that encoded reward or effort signals, we implemented the first GLM

(GLM1) which included 8 conditions: cue 1, cue 2, choice (the period after both pieces of

information have been presented and participants may make a choice), and response (the

time at which participant's make a choice) divided by order of presentation (effort first or

reward first). The first three phases were associated with two parametric modulators: the

reward magnitude and effort of the chosen option.

To further investigate and identify areas that encoded subjective value as well as the

integration of effort and reward information, we implemented a second GLM. The second

GLM (GLM2) was identical to the first, except that parametric modulators were replaced

by predicted reward and effort at Cue 1 (calculated with a sliding window analysis) and

subjective value estimates of the chosen option at Cue 2.

Lastly, a third GLM (GLM3) aimed to identify areas that encoded prediction as well as

an unsigned prediction error. It was identical to the first except that the parametric

modulators were replaced by predicted subjective value as determined by our sliding

window analysis at cue 1 as well as SVPE at cue 2.

For whole-brain analyses, we used a FWE cluster-corrected threshold of $p < 0.05$ (using a

cluster-defining threshold of $p < 0.005$ and a cluster threshold of 20 voxels). Beta values

were extracted from ROIs as well as from various defined regions of the medial

prefrontal cortex[43] as well as the insula[42].

References

1   Rangel, A., Camerer, C. & Montague, P. R. A framework for studying the neurobiology of value-based decision making. *Nat Rev Neurosci* **9**, 545-556, doi:10.1038/nrn2357 (2008).

2   Massar, S. A., Libedinsky, C., Weiyan, C., Huettel, S. A. & Chee, M. W. Separate and overlapping brain areas encode subjective value during delay and effort discounting. *Neuroimage* **120**, 104-113, doi:10.1016/j.neuroimage.2015.06.080 (2015).

3   Kable, J. W. & Glimcher, P. W. The neurobiology of decision: consensus and controversy. *Neuron* **63**, 733-745, doi:10.1016/j.neuron.2009.09.003 (2009).

4   Treadway, M. T., Buckholtz, J. W., Schwartzman, A. N., Lambert, W. E. & Zald, D. H. Worth the 'EEfRT'? The effort expenditure for rewards task as an objective measure of motivation and anhedonia. *PLoS One* **4**, e6598, doi:10.1371/journal.pone.0006598 (2009).

5   Kool, W. & Botvinick, M. A labor/leisure tradeoff in cognitive control. *J Exp Psychol Gen* **143**, 131-141, doi:10.1037/a0031048 (2014).

6   Walton, M. E. & Mars, R. B. Probing human and monkey anterior cingulate cortex in variable environments. *Cogn Affect Behav Neurosci* **7**, 413-422 (2007).

7   Walton, M. E. *et al.* Comparing the role of the anterior cingulate cortex and 6-hydroxydopamine nucleus accumbens lesions on operant effort-based decision making. *Eur J Neurosci* **29**, 1678-1691, doi:10.1111/j.1460-9568.2009.06726.x (2009).

8   Walton, M. E., Croxson, P. L., Rushworth, M. F. & Bannerman, D. M. The

        mesocortical dopamine projection to anterior cingulate cortex plays no role in

        guiding effort-related decisions. *Behav Neurosci* **119**, 323-328, doi:10.1037/0735-

        7044.119.1.323 (2005).

9   Walton, M. E., Croxson, P. L., Behrens, T. E., Kennerley, S. W. & Rushworth, M.

        F. Adaptive decision making and value in the anterior cingulate cortex.

        Neuroimage **36 Suppl 2**, T142-154, doi:10.1016/j.neuroimage.2007.03.029

        (2007).

10   Walton, M. E., Bannerman, D. M., Alterescu, K. & Rushworth, M. F. Functional

        specialization within medial frontal cortex of the anterior cingulate for evaluating

        effort-related decisions. *J Neurosci* **23**, 6475-6479 (2003).

11   Rudebeck, P. H., Buckley, M. J., Walton, M. E. & Rushworth, M. F. A role for

        the macaque anterior cingulate gyrus in social valuation. *Science* **313**, 1310-1312,

        doi:10.1126/science.1128197 (2006).

12   Rudebeck, P. H. *et al.* Frontal cortex subregions play distinct roles in choices

        between actions and stimuli. *J Neurosci* **28**, 13775-13785,

        doi:10.1523/JNEUROSCI.3541-08.2008 (2008).

13   Wallis, J. D. & Kennerley, S. W. Contrasting reward signals in the orbitofrontal

        cortex and anterior cingulate cortex. *Ann N Y Acad Sci* **1239**, 33-42,

        doi:10.1111/j.1749-6632.2011.06277.x (2011).

14   Kennerley, S. W., Walton, M. E., Behrens, T. E., Buckley, M. J. & Rushworth,

        M. F. Optimal decision making and the anterior cingulate cortex. *Nat Neurosci* **9**,

        940-947, doi:10.1038/nn1724 (2006).

15   Kennerley, S. W. & Wallis, J. D. Evaluating choices by single neurons in the

         frontal lobe: outcome value encoded across multiple decision variables. *Eur J*

         Neurosci **29**, 2061-2073, doi:10.1111/j.1460-9568.2009.06743.x (2009).

16   Kennerley, S. W. & Wallis, J. D. Encoding of reward and space during a working

         memory task in the orbitofrontal cortex and anterior cingulate sulcus. *J*

         Neurophysiol **102**, 3352-3364, doi:10.1152/jn.00273.2009 (2009).

17   Kennerley, S. W., Behrens, T. E. & Wallis, J. D. Double dissociation of value

         computations in orbitofrontal and anterior cingulate neurons. *Nat Neurosci* **14**,

         1581-1589, doi:10.1038/nn.2961 (2011).

18   Schmidt, L., Lebreton, M., Clery-Melin, M. L., Daunizeau, J. & Pessiglione, M.

         Neural mechanisms underlying motivation of mental versus physical effort. *PLoS*

         Biol **10**, e1001266, doi:10.1371/journal.pbio.1001266 (2012).

19   Prevost, C., Pessiglione, M., Metereau, E., Clery-Melin, M. L. & Dreher, J. C.

         Separate valuation subsystems for delay and effort decision costs. *J Neurosci* **30**,

         14080-14090, doi:10.1523/JNEUROSCI.2752-10.2010 (2010).

20   McGuire, J. T. & Botvinick, M. M. Prefrontal cortex, cognitive control, and the

         registration of decision costs. *Proc Natl Acad Sci U S A* **107**, 7922-7926,

         doi:10.1073/pnas.0910662107 (2010).

21   Jansma, J. M., Ramsey, N. F., de Zwart, J. A., van Gelderen, P. & Duyn, J. H.

         fMRI study of effort and information processing in a working memory task. *Hum*

         Brain Mapp **28**, 431-440, doi:10.1002/hbm.20297 (2007).

22   Vassena, E., Holroyd, C. B. & Alexander, W. H. Computational Models of

        Anterior Cingulate Cortex: At the Crossroads between Prediction and Effort.

        Front Neurosci **11**, 316, doi:10.3389/fnins.2017.00316 (2017).

23   Alexander, W. H. & Brown, J. W. A general role for medial prefrontal cortex in

        event prediction. *Front Comput Neurosci* **8**, 69, doi:10.3389/fncom.2014.00069

        (2014).

24   Alexander, W. H. & Brown, J. W. Medial prefrontal cortex as an action-outcome

        predictor. *Nat Neurosci* **14**, 1338-1344, doi:10.1038/nn.2921 (2011).

25   Palminteri, S. *et al.* Critical roles for anterior insula and dorsal striatum in

        punishment-based avoidance learning. *Neuron* **76**, 998-1009,

        doi:10.1016/j.neuron.2012.10.017 (2012).

26   Preuschoff, K., Quartz, S. R. & Bossaerts, P. Human insula activation reflects risk

        prediction errors as well as risk. *J Neurosci* **28**, 2745-2752,

        doi:10.1523/JNEUROSCI.4286-07.2008 (2008).

27   Rushworth, M. F. & Behrens, T. E. Choice, uncertainty and value in prefrontal

        and cingulate cortex. *Nat Neurosci* **11**, 389-397, doi:10.1038/nn2066 (2008).

28   Rushworth, M. F., Behrens, T. E., Rudebeck, P. H. & Walton, M. E. Contrasting

        roles for cingulate and orbitofrontal cortex in decisions and social behaviour.

        Trends Cogn Sci **11**, 168-176, doi:10.1016/j.tics.2007.01.004 (2007).

29   Rushworth, M. F., Kolling, N., Sallet, J. & Mars, R. B. Valuation and decision-

        making in frontal cortex: one or many serial or parallel systems? *Curr Opin

        Neurobiol* **22**, 946-955, doi:10.1016/j.conb.2012.04.011 (2012).

30   Shenhav, A. & Botvinick, M. Uncovering a missing link in anterior cingulate research. *Neuron* **85**, 455-457, doi:10.1016/j.neuron.2015.01.020 (2015).

31   Shenhav, A., Botvinick, M. M. & Cohen, J. D. The expected value of control: an integrative theory of anterior cingulate cortex function. *Neuron* **79**, 217-240, doi:10.1016/j.neuron.2013.07.007 (2013).

32   Shenhav, A., Cohen, J. D. & Botvinick, M. M. Dorsal anterior cingulate cortex and the value of control. *Nat Neurosci* **19**, 1286-1291, doi:10.1038/nn.4384 (2016).

33   Shenhav, A., Straccia, M. A., Botvinick, M. M. & Cohen, J. D. Dorsal anterior cingulate and ventromedial prefrontal cortex have inverse roles in both foraging and economic choice. *Cogn Affect Behav Neurosci* **16**, 1127-1139, doi:10.3758/s13415-016-0458-8 (2016).

34   Shenhav, A., Straccia, M. A., Cohen, J. D. & Botvinick, M. M. Anterior cingulate engagement in a foraging context reflects choice difficulty, not foraging value. *Nat Neurosci* **17**, 1249-1254, doi:10.1038/nn.3771 (2014).

35   Holroyd, C. B. *et al.* Dorsal anterior cingulate cortex shows fMRI response to internal and external error signals. *Nat Neurosci* **7**, 497-498, doi:10.1038/nn1238 (2004).

36   Botvinick, M. M., Braver, T. S., Barch, D. M., Carter, C. S. & Cohen, J. D. Conflict monitoring and cognitive control. *Psychol Rev* **108**, 624-652 (2001).

37   Rangel, A. & Hare, T. Neural computations associated with goal-directed choice. *Curr Opin Neurobiol* **20**, 262-270, doi:10.1016/j.conb.2010.03.001 (2010).

38   Kolling, N., Behrens, T. E., Mars, R. B. & Rushworth, M. F. Neural mechanisms of foraging. *Science* **336**, 95-98, doi:10.1126/science.1216930 (2012).

39   Verguts, T., Vassena, E. & Silvetti, M. Adaptive effort investment in cognitive and physical tasks: a neurocomputational model. *Front Behav Neurosci* **9**, 57, doi:10.3389/fnbeh.2015.00057 (2015).

40   Croxson, P. L., Walton, M. E., O'Reilly, J. X., Behrens, T. E. & Rushworth, M. F. Effort-based cost-benefit valuation and the human brain. *J Neurosci* **29**, 4531-4541, doi:10.1523/JNEUROSCI.4515-08.2009 (2009).

41   Klein-Flugge, M. C., Kennerley, S. W., Saraiva, A. C., Penny, W. D. & Bestmann, S. Behavioral modeling of human choices reveals dissociable effects of physical effort and temporal delay on reward devaluation. *PLoS Comput Biol* **11**, e1004116, doi:10.1371/journal.pcbi.1004116 (2015).

42   Chang, L. J., Yarkoni, T., Khaw, M. W. & Sanfey, A. G. Decoding the role of the insula in human cognition: functional parcellation and large-scale reverse inference. *Cereb Cortex* **23**, 739-749, doi:10.1093/cercor/bhs065 (2013).

43   de la Vega, A., Chang, L. J., Banich, M. T., Wager, T. D. & Yarkoni, T. Large-Scale Meta-Analysis of Human Medial Frontal Cortex Reveals Tripartite Functional Organization. *J Neurosci* **36**, 6553-6562, doi:10.1523/JNEUROSCI.4402-15.2016 (2016).

44   Pauli, W. M., O'Reilly, R. C., Yarkoni, T. & Wager, T. D. Regional specialization within the human striatum for diverse psychological functions. *Proc Natl Acad Sci U S A* **113**, 1907-1912, doi:10.1073/pnas.1507610113 (2016).

45   Chong, T. T. *et al.* Neurocomputational mechanisms underlying subjective

        valuation of effort costs. *PLoS Biol* **15**, e1002598,

        doi:10.1371/journal.pbio.1002598 (2017).

46   Heilbronner, S. R. & Hayden, B. Y. Dorsal Anterior Cingulate Cortex: A Bottom-

        Up View. *Annu Rev Neurosci* **39**, 149-170, doi:10.1146/annurev-neuro-070815-

        013952 (2016).

47   Lebreton, M., Jorge, S., Michel, V., Thirion, B. & Pessiglione, M. An automatic

        valuation system in the human brain: evidence from functional neuroimaging.

        Neuron **64**, 431-439, doi:10.1016/j.neuron.2009.09.040 (2009).

48   Boorman, E. D. & Rushworth, M. F. Conceptual representation and the making of

        new decisions. *Neuron* **63**, 721-723, doi:10.1016/j.neuron.2009.09.014 (2009).

49   Rudebeck, P. H., Walton, M. E., Smyth, A. N., Bannerman, D. M. & Rushworth,

        M. F. Separate neural pathways process different decision costs. *Nat Neurosci* **9**,

        1161-1168, doi:10.1038/nn1756 (2006).

50   Kurniawan, I. T. *et al.* Choosing to make an effort: the role of striatum in

        signaling physical effort of a chosen action. *J Neurophysiol* **104**, 313-321,

        doi:10.1152/jn.00027.2010 (2010).

51   Schouppe, N., Demanet, J., Boehler, C. N., Ridderinkhof, K. R. & Notebaert, W.

        The role of the striatum in effort-based decision-making in the absence of reward.

        J Neurosci **34**, 2148-2154, doi:10.1523/JNEUROSCI.1214-13.2014 (2014).

52   Botvinick, M. M., Huffstetler, S. & McGuire, J. T. Effort discounting in human

        nucleus accumbens. *Cogn Affect Behav Neurosci* **9**, 16-27,

        doi:10.3758/CABN.9.1.16 (2009).

53   Salamone, J. D., Correa, M., Mingote, S. & Weber, S. M. Nucleus accumbens dopamine and the regulation of effort in food-seeking behavior: implications for studies of natural motivation, psychiatry, and drug abuse. *J Pharmacol Exp Ther* **305**, 1-8, doi:10.1124/jpet.102.035063 (2003).

54   Klein-Flugge, M. C., Kennerley, S. W., Friston, K. & Bestmann, S. Neural Signatures of Value Comparison in Human Cingulate Cortex during Decisions Requiring an Effort-Reward Trade-off. *J Neurosci* **36**, 10002-10015, doi:10.1523/JNEUROSCI.0292-16.2016 (2016).

55   Bonnelle, V. *et al.* Characterization of reward and effort mechanisms in apathy. *J Physiol Paris* **109**, 16-26, doi:10.1016/j.jphysparis.2014.04.002 (2015).

56   Treadway, M. T. & Zald, D. H. Parsing Anhedonia: Translational Models of Reward-Processing Deficits in Psychopathology. *Curr Dir Psychol Sci* **22**, 244-249, doi:10.1177/0963721412474460 (2013).

57   Treadway, M. T., Bossaller, N. A., Shelton, R. C. & Zald, D. H. Effort-based decision-making in major depressive disorder: a translational model of motivational anhedonia. *J Abnorm Psychol* **121**, 553-558, doi:10.1037/a0028813 (2012).

58   Fervaha, G. *et al.* Incentive motivation deficits in schizophrenia reflect effort computation impairments during cost-benefit decision-making. *J Psychiatr Res* **47**, 1590-1596, doi:10.1016/j.jpsychires.2013.08.003 (2013).

59   Brainard, D. H. The Psychophysics Toolbox. *Spat Vis* **10**, 433-436 (1997).

60   Hartmann, M. N., Hager, O. M., Tobler, P. N. & Kaiser, S. Parabolic discounting

        of monetary rewards by physical effort. *Behav Processes* **100**, 192-196,

        doi:10.1016/j.beproc.2013.09.014 (2013).

61   Phillips, P. E., Walton, M. E. & Jhou, T. C. Calculating utility: preclinical

        evidence for cost-benefit analysis by mesolimbic dopamine. *Psychopharmacology

        (Berl)* **191**, 483-495, doi:10.1007/s00213-006-0626-6 (2007).

62   Frederick, S., Loewenstein, G. & O'Donoghue, T. Time discounting and time

        preference: a critical review. *Journal of Economic Literature* **40**, 351-401 (2002).

63   Green, L., Fry, A. F. & Myerson, J. Discounting of delayed rewards: a life span

        comparison. *Psychological Science* **5**, 33-36 (1994).

64   Sugiwaka, H. & Okouchi, H. Reformative self-control and discounting of reward

        value by delay or effort. *Japanese Psychological Research* **46**, 1-9 (2004).

65   Gureckis, T. M. & Love, B. C. Short-term gains, long-term pains: how cues about

        state aid learning in dynamic environments. *Cognition* **113**, 293-313,

        doi:10.1016/j.cognition.2009.03.013 (2009).

66   Akaike, H. A new look at the statistical model identification. *IEEE Transactions

        on Automatic Control* **19**, 716-723 (1974).
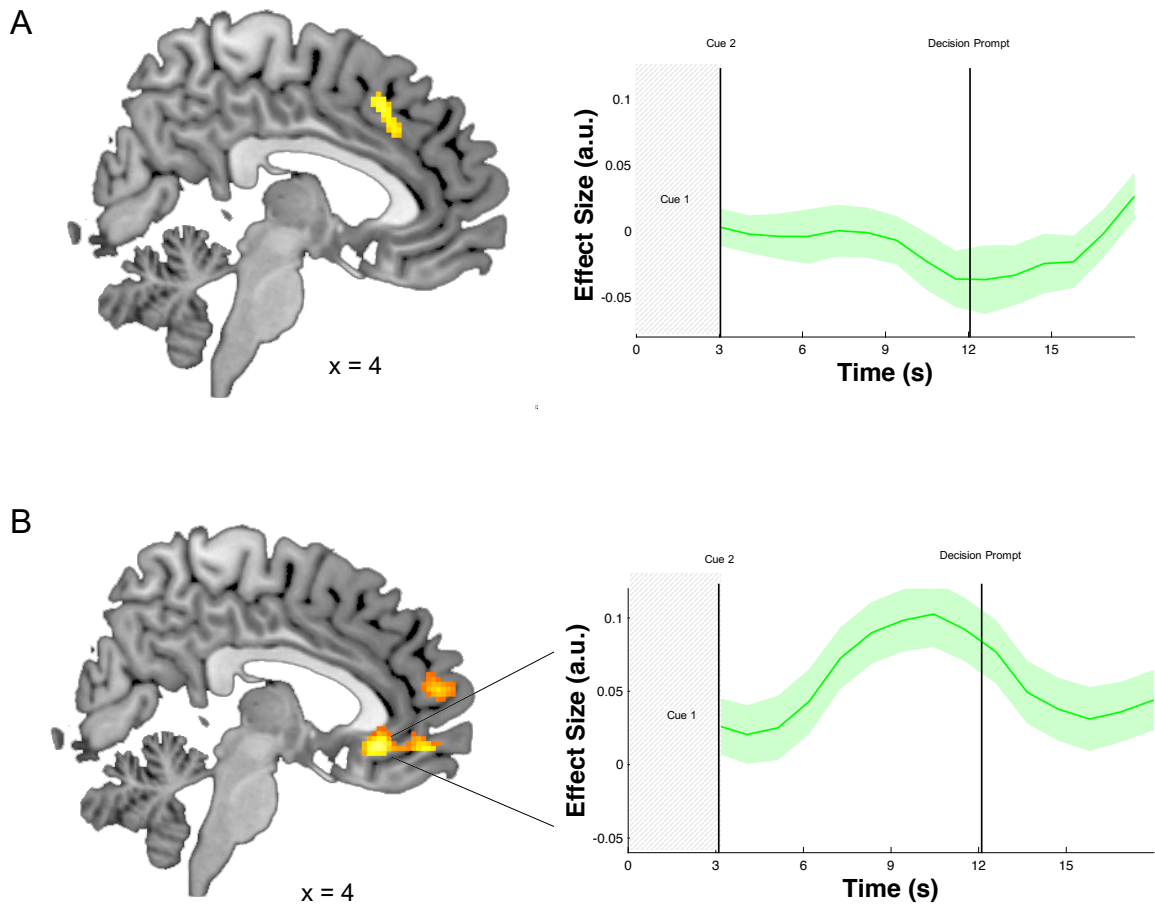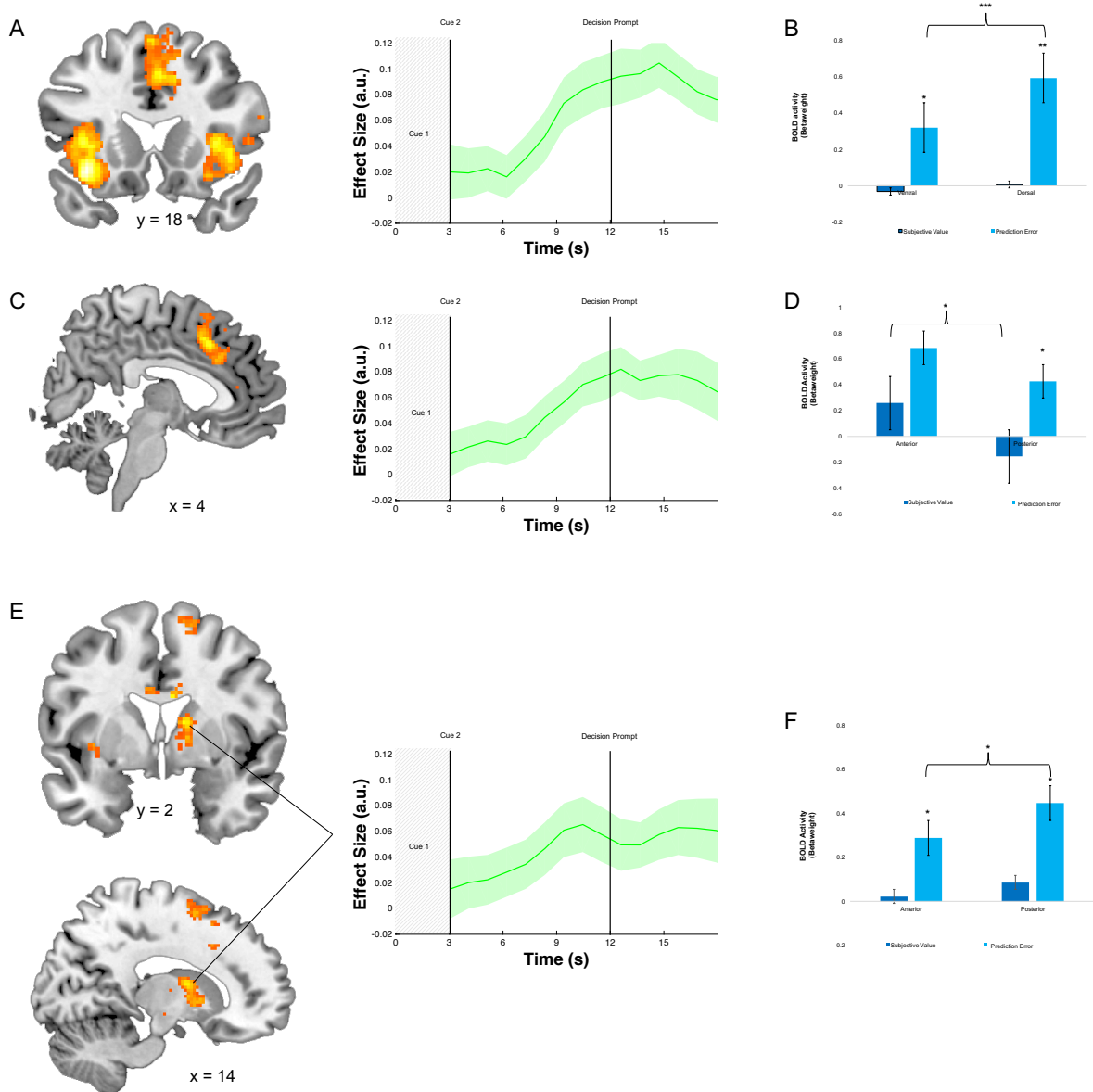
FIGURES

FIGURE 1
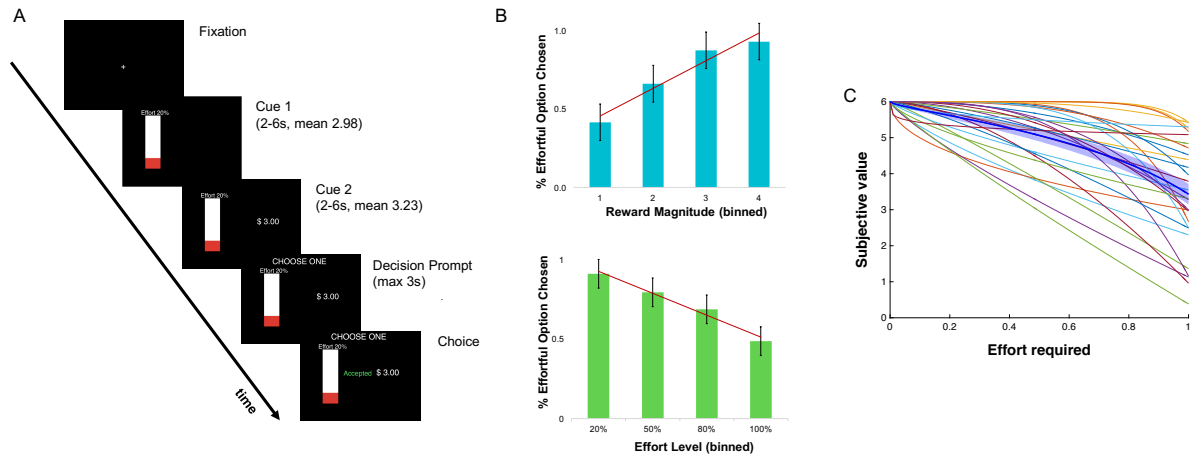
Figure 1.
(A) Schematic of experimental task design. This image shows the timeline of a trial in which effort and reward information are presented sequentially. This is an example of an "Effort first" trial. Each trial began with the presentation of a fixation cross, followed by the Cue 1 phase in which one piece of information was presented (either effort level or reward magnitude). After 2-6s, the second piece of information was presented (Cue 2). After an additional 2-6s, participants saw a Decision prompt which prompted them to make a choice between the Effort Option presented and the No Effort option that always paid $1.00. They were required to make their selection within 3s. Following their selection their choice would be presented to them during the Choice phase. **(B)** Proportion of effortful choices based upon effort level and reward magnitude. Participants chose more effortful options as reward increased and as effort decreased. Error bars are all S.E.M. **(C)** Individual and group average subjective value curves based on the results of our computational model. The group average is shown as the dark blue line with shading around it that represents the standard error. The remaining colored lines each reflect a single participant, demonstrating individual differences in discounting.

FIGURE 2

Figure 2.
(A) Increased BOLD signal in dACC in response to subjective value discounting. Effect size plot demonstrates the negative relationship between BOLD activity and subjective value magnitude in dACC. **(B)** Increased BOLD signal in vmPFC in response to subjective value magnitude. Effect size plot demonstrates the positive relationship between BOLD activity and subjective value magnitude in vmPFC.

FIGURE 3

Figure 3.
(A) Increased BOLD activity in bilateral anterior insula (AI) in response to unsigned subjective value prediction error (SVPE) generation. Effect size plot demonstrates this positive relationship between BOLD signal and SVPE. **(B)** BOLD activity in insula is significantly greater in response to SVPE than subjective value. Further, within prediction error, dorsal insula activity is significantly stronger than ventral insula. **(C)** Increased BOLD activity in dACC in response to unsigned SVPE. Effect size plot demonstrates this positive relationship between BOLD signal and prediction error encoding. **(D)** BOLD activity in anterior dACC is significantly stronger than posterior dACC for subjective value. In posterior dACC, greater BOLD activity was observed in

response to SVPE than subjective value alone. **(E)** Increased BOLD activity in caudate in response to unsigned SVPE. Effect size plot demonstrates this positive relationship between BOLD signal and prediction error encoding. **(F)** BOLD activity in caudate is significantly greater in response to SVPE than subjective value. Further, posterior caudate is more active than anterior caudate for prediction error encoding.
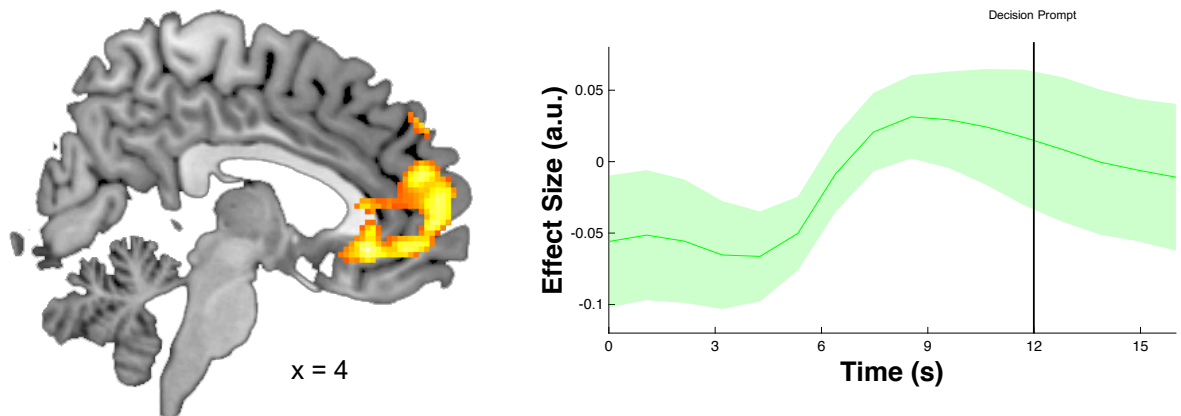*$p<0.05$; ** $p<0.005$; ***$p<0.001$*

FIGURE 4

Figure 4. Increased BOLD activity at Cue 1 in response to predicted reward in vmPFC. Effect size plot illustrates positive relationship between BOLD signal and predicted reward magnitude.

TABLES

Table 1. Model Fits

	k	*β*	*p*	*V*$_i$	AIC
Fixed Probability	0.34	-	-	1	102.27
Linear	2.32	3.67	-	2	44.39
Quadratic	2.81	5	-	2	43.46
Hyperbolic	2.35	7.33	-	2	45.06
Two-Parameter Power	2.57	9.92	2.71	3	39.52

k and p are free parameters; $β$ is the inverse temperature parameter; V_i is the number of free parameters, which indicated overall model complexity; AIC is Akiake's Information Criterion.

SUPPLEMENTAL METHODS

Indifference Point Estimation and Choice Difficulty Model

In addition to estimating subjective value, we modeled indifference points for each

subject as a means of identifying choices that were likely easy to make (i.e., far above or

below a subject's indifference point) vs. relatively difficult to make (i.e., close to a

subject's indifference point). We determined points of subjective indifference (that is the

points at which the choices were most difficult) at each stage of the task based on

participants' choices. The choices performed for each of the four levels of effort were

plotted as a function of the magnitude of the alternative, non-effortful option. A simple

sigmoid was fitted using equation S1 below, and the indifference point was defined as the

reward magnitude (on x) at which the sigmoid crossed y = 0.5, which corresponds to α; β

is the slope:

$$\frac{1}{1 + e^{-\beta(x-\alpha)}} \hspace{4cm} Eq. S1$$

To identify areas the encoded choice difficulty, we implemented an additional GLM

(GLMS1). This model divided trials based on the difference between the reward

presented and participants' indifference points for similar trial types. Trials where the

reward required was close to the indifference point were determined to be more difficult

trials whereas trials where the reward was further away from the indifference point (in

either direction) were labeled as easier choice trials. This GLM included 8 conditions:

low and high difficulty trials divided by order presentation at both the cue 1 and cue 2

phases.

Subjective Value Prediction Error Additional Methods

Estimates of expected subjective value at Cue 1 ($SV_{predicted}$) were calculated using a

sliding window analysis of previously-experienced subjective values of the same trial

type. The value of $SV_{predicted}$ on each trial was derived from the Cue 1 stimulus (i.e.

reward bin or level of effort) and recent subjective values of trials from the same reward

bin or effort level shown at Cue 1. Subjective values for previous trials were calculated

using the two-parameter power function (Equation 1) and each participant's best-fitting

parameters. The sliding windows of subjective values for each reward bin ($1.25-2.39,

$2.40-3.49, $3.50-4.60, >$4.60) and effort level (20%, 50%, 80%, 100%) were initiated

at [4; 1] to begin each window with a realistic range of subjective values. After each trial,

the sliding windows for the cue information in the current trial were updated with the

model-derived SV. For example, on a trial with a reward of 4.20, required effort of 50%,

and model-derived subjective value of $3.30, the sliding windows for the $3.50-4.60

reward bin and 50% effort level would both be updated with the SV of $3.30 to be used

in calculating the predicted SV on future trials with the same reward bin or effort level at

Cue 1. The $SV_{predicted}$ on a trial where the Cue 1 information was 50% was calculated by

averaging the most five most recent values in the 50% effort level sliding window (or all

existing values if five trials had not yet been encountered).

Binned Trial Analysis:

An additional GLM (GLMS2) sought to investigate how neural regions encoding

subjective where influence by choice. This model was a binned analysis model,

consisting of 4 bins. The first 3 bins were based on trials where the effortful option was

chosen, and were divided based on the magnitude of the subjective value of the chosen

option for those trials. The fourth bin was for trials where the effortful option was not

chosen. A linear contrast was used to investigate how neural regions were tracking

subjective value across both choice conditions.

SUPPLEMENTAL RESULTS

Choice Difficulty

Some studies have suggested that dACC engagement during value-based decision-

making is due to the relative ease or difficulty with which one arrives at a decision[1-3].

When the subjective value of two options is far apart, deciding between them is relatively

easy; when two options have very similar subjective values (i.e., near a subject's

indifference point), choice difficulty may increase. Participants made significantly less

effortful choices for trials that were close to their indifference point compared to those

that were not ($t_{(27)=}$ -4.58 ; $p = 9.34 \times 10^{-5}$).

We also confirmed that difficult choice trials as we defined them had slower reaction

times than easier choice trials, a marker of choice difficulty[3] ($t_{(27)} = 2.52$; $p = 0.018$).

Given the ongoing debate as to whether dACC activity tracks unchosen option values as

opposed to choice difficulty[1-9], we were next interested in investigating its role in choice

computations and evaluation. We began our investigation by comparing difficult and easy

choice trials (GLM3), expecting that if dACC encoded choice difficulty, we would see

greater activation for trials where the value of the Effort Option approaches the

individual's indifference point. We observed greater dACC activity for more difficult

trials compared to easier choice trials (x = 4, y = 20, z = 44, t = 5.20, cluster corrected

pFWE < 0.001). Additionally, during more difficult trials, dACC recruited dlPFC (x =

46, y = 34, z = 32, t = 5.00, cluster corrected pFWE = 0.004), suggesting this circuit's

involvement in choice difficulty (**Supplemental Figure S2**). It is important to note that

because we modeled choice difficulty pre-choice (at Cue 2), our BOLD signal findings

were not influenced by our difference in reaction times between the two types of choice

trials (i.e. easy vs. difficult). Notably, dACC response to both SV and choice difficulty

has been previously reported, but more recently, debate has arisen as to whether SV

encoding in the dACC may be wholly reducible to choice difficulty. Our study design

was not optimized to address this particular question, but we observed that SV and choice

difficulty were highly collinear (mean r^2 = 0.49) (**Supplemental Figure S3C**). As a

result, the current study was unable to fully disambiguate between dACC involvement in

SV and choice difficulty.

Subjective Value Extended

An additional question was whether our subjective value findings were driven by

subjective value itself, or by choice. To identify this, we additionally examined chosen

SV *within* trials where the effortful option was selected and again observed vmPFC and

dACC activity. To further understand how these regions were tracking subjective value,

we implemented a binned trial analysis (GLMS2). Results of this analysis demonstrated a

linear relationship between dACC and caudate and subjective value. This analysis also

helped us understand if this linear relationship held across chosen and unchosen options.

We observed the greatest BOLD activity in dACC for trials with the lowest subjective

value, which also happened to be trials where participants chose the non-effortful option.

In this way and consistent with previous findings, we see dACC track linearly with

subjective value, but also encode and signal a behavioral set shift away from the Effort

Option.

Supplemental References

1   Shenhav, A., Cohen, J. D. & Botvinick, M. M. Dorsal anterior cingulate cortex
        and the value of control. *Nat Neurosci* **19**, 1286-1291, doi:10.1038/nn.4384
        (2016).

2   Shenhav, A., Straccia, M. A., Botvinick, M. M. & Cohen, J. D. Dorsal anterior
        cingulate and ventromedial prefrontal cortex have inverse roles in both foraging
        and economic choice. *Cogn Affect Behav Neurosci* **16**, 1127-1139,
        doi:10.3758/s13415-016-0458-8 (2016).

3   Shenhav, A., Straccia, M. A., Cohen, J. D. & Botvinick, M. M. Anterior cingulate
        engagement in a foraging context reflects choice difficulty, not foraging value.
        Nat Neurosci **17**, 1249-1254, doi:10.1038/nn.3771 (2014).

4   Alexander, W. H. & Brown, J. W. Medial prefrontal cortex as an action-outcome
        predictor. *Nat Neurosci* **14**, 1338-1344, doi:10.1038/nn.2921 (2011).

5   Alexander, W. H. & Brown, J. W. A general role for medial prefrontal cortex in
        event prediction. *Front Comput Neurosci* **8**, 69, doi:10.3389/fncom.2014.00069
        (2014).

6   Kolling, N., Behrens, T. E., Mars, R. B. & Rushworth, M. F. Neural mechanisms
        of foraging. *Science* **336**, 95-98, doi:10.1126/science.1216930 (2012).

7   Shenhav, A. & Botvinick, M. Uncovering a missing link in anterior cingulate
        research. *Neuron* **85**, 455-457, doi:10.1016/j.neuron.2015.01.020 (2015).

8   Shenhav, A., Botvinick, M. M. & Cohen, J. D. The expected value of control: an
        integrative theory of anterior cingulate cortex function. *Neuron* **79**, 217-240,
        doi:10.1016/j.neuron.2013.07.007 (2013).

9   Vassena, E., Holroyd, C. B. & Alexander, W. H. Computational Models of

         Anterior Cingulate Cortex: At the Crossroads between Prediction and Effort.

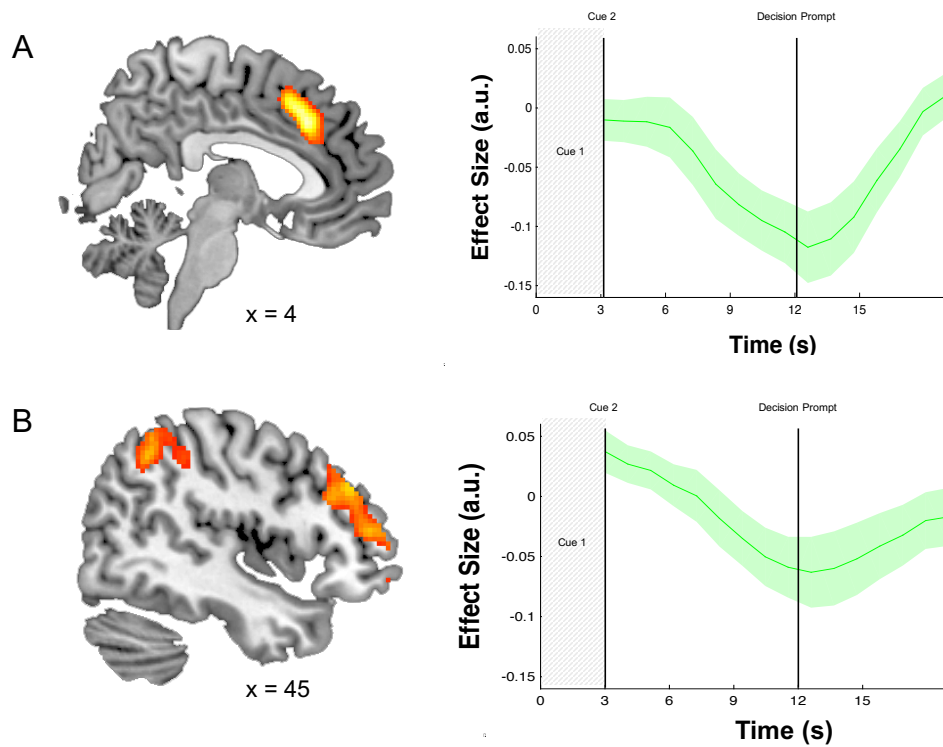   *Front Neurosci* **11**, 316, doi:10.3389/fnins.2017.00316 (2017).

SUPPLEMENTAL FIGURES

SUPPLEMENTAL FIGURE 1

y = 18   x = 4

y = 2
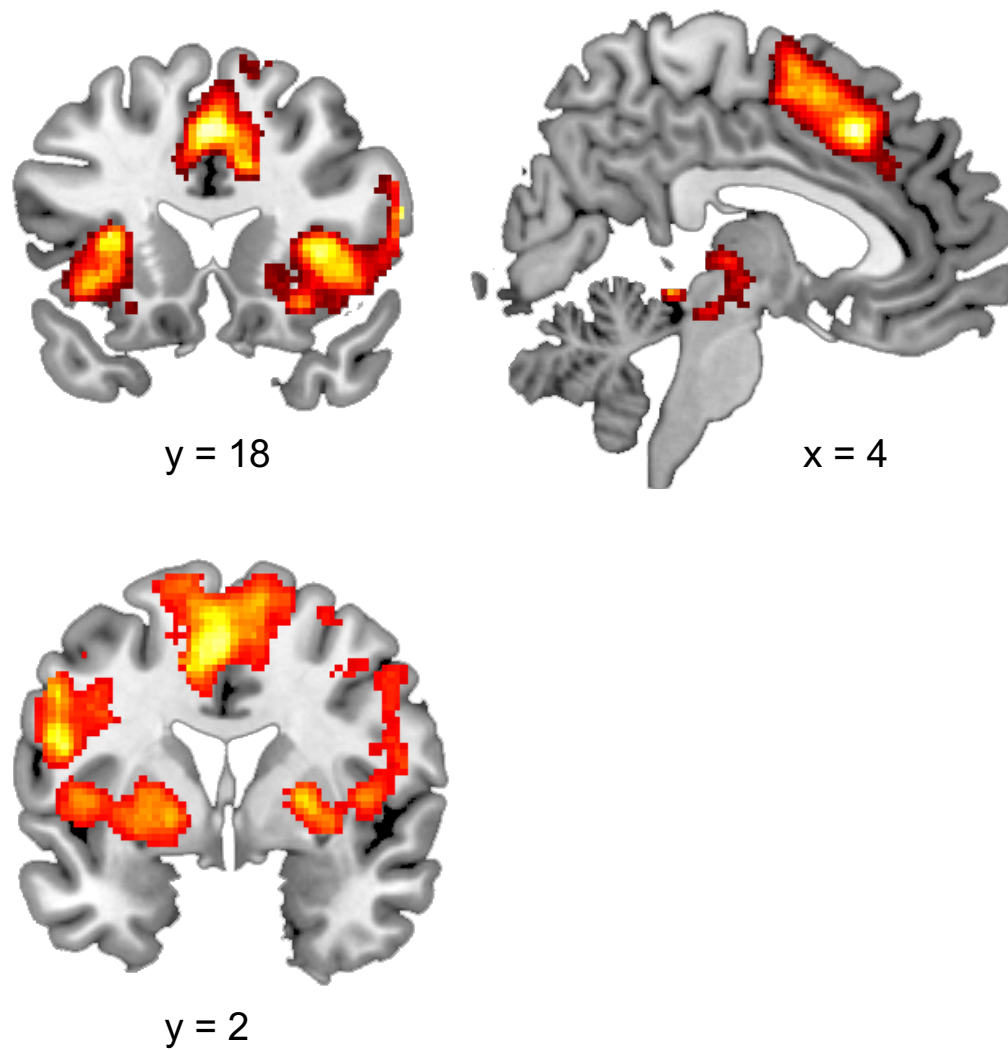
Figure S1.
Increased BOLD signal in dACC, putamen, insula, and SMA at Cue 2.

SUPPLEMENTAL FIGURE 2

Figure S2.
(A) Increased BOLD signal in dACC in response to increasing choice difficulty. Effect size plot demonstrates the negative relationship between BOLD activity and easy choice trials in dACC. **(B)** Increased BOLD signal in dlPFC in response to increasing choice difficulty. Effect size plot demonstrates the negative relationship between BOLD activity and easy choice trials in dlPFC.

SUPPLEMENTAL FIGURE 3
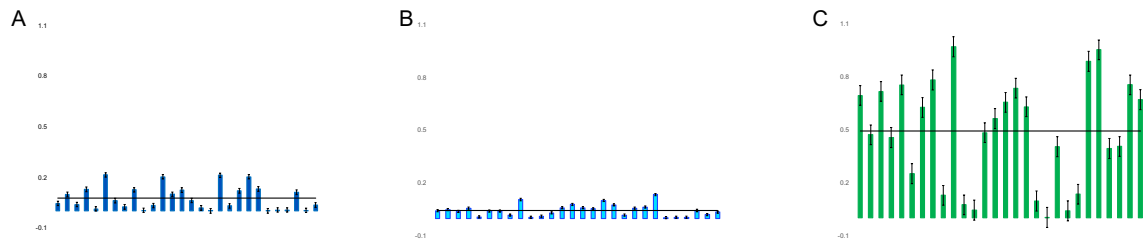
Figure S3.
(A) Average correlation (R^2) between model-based regressors of unsigned prediction error and subjective value per individual. Group average R^2 ($R^2 = 0.08$) is shown as black horizontal line. **(B)** Average correlation (R^2) between model-based regressors of unsigned prediction error and choice difficulty per individual. Group average R^2 ($R^2 = 0.04$) is shown as black horizontal line. **(C)** Average correlation (R^2) between model-based regressors of choice difficulty and subjective value per individual. Group average R^2 ($R^2 = 0.49$) is shown as black horizontal line.

SUPPLEMENTAL TABLES

Table S1. Demographics

N	28
Age (yrs)	
Mean	20.18
S.D	2.06
Range	18-25
Race	
American Indian / Alaska Native	0
Asian	13
Black / African-American	1
White	14
Ethnicity	
Hispanic / Latino	3
Not Hispanic / Latino	25